

8. DATA REPORT: LATE PLEISTOCENE– HOLOCENE SEDIMENTATION ALONG THE UPPER SLOPE OF THE GREAT AUSTRALIAN BIGHT¹

Albert C. Hine,² Gregg R. Brooks,³ David Mallinson,⁴
Charlotte A. Brunner,⁵ Noel P. James,⁶ David A. Feary,⁷
Ann E. Holbourn,⁸ Tina M. Drexler,³ and Peter Howd²

ABSTRACT

This data report presents sedimentological (grain size) and geochemical (X-ray diffraction, total organic carbon, accelerator mass spectrometry radiocarbon, and percent carbonate) information obtained from the western transect (Sites 1132, 1130, and 1134) and the eastern transect (Sites 1129, 1131, and 1127) in the Great Australian Bight during Leg 182. The purpose is to quantify changing rates of sediment accumulation and changes in sediment type from the late Pleistocene and Holocene, in order to relate these changes to the well-known sea level curve that exists for this time frame. Ultimately, these data can be used to more effectively interpret lithologic variations deeper in the Pleistocene succession, which most likely represent orbitally forced sea level events.

INTRODUCTION

One of the key preliminary results of Ocean Drilling Program (ODP) Leg 182 was the surprising thickness of the Pleistocene succession in the upper slope—up to 550 m resulting from sedimentation rates as high as 440 m/m.y. (Feary, Hine, Malone, et al., 2000). This is comparable to Quaternary sedimentation rates in warm-water settings of well-known carbonate depositional systems such as west Florida (Mullins et

¹Hine, A.C., Brooks, G.R., Mallinson, D., Brunner, C.A., James, N.P., Feary, D.A., Holbourn, A.E., Drexler, T.M., and Howd, P., 2002. Data report: Late Pleistocene–Holocene sedimentation along the upper slope of the Great Australian Bight. In Hine, A.C., Feary, D.A., and Malone, M.J. (Eds.), *Proc. ODP, Sci. Results*, 182, 1–24 [Online]. Available from World Wide Web: <http://www-odp.tamu.edu/publications/182_SR/VOLUME/CHAPTERS/009.PDF>. [Cited YYYY-MM-DD]

²College of Marine Science, University of South Florida, St. Petersburg FL 33701, USA. Correspondence author: hine@marine.usf.edu

³Department of Marine Science, Eckerd College, St. Petersburg FL 33711, USA.

⁴Department of Geology, East Carolina University, Greenville NC 27834, USA.

⁵Department of Marine Science, University of Southern Mississippi, John C. Stennis Space Center MS 39529, USA.

⁶Department of Geological Sciences, Queens University, Kingston ON K7L 3N6, Canada.

⁷National Academy of Sciences, Washington DC, USA.

⁸IMAGES, Institut für Geowissenschaften, Christian Albrechts Universität, 24118 Kiel, Germany.

al., 1988a, 1988b), the Bahamas (Eberli, Swart, Malone, et al., 1997), or the Nicaraguan Rise (Glaser et al., 1991; see “Summary” in James, 1997). In fact, this cool-water carbonate setting produced some of the highest sustained accumulation rates recorded over significant (i.e., $>10^6$ yr) lengths of time.

As shown by the stable isotopic data from benthic foraminifers (Holbourn et al., in press), the Pleistocene succession at Sites 1129, 1131, and 1132 contains variations that can be tied to the Specmap stack (Imbrie et al., 1984; Martinson et al., 1987) indicating that an orbitally forced signal exists. Within a thick stratigraphic succession that contains an orbitally forced isotopic signal, sedimentary cycles containing a distinct and predictable facies architecture may dominate.

PROBLEM DEVELOPMENT

As best illustrated through borehole logging and seismic data, the facies architecture is not monolithic but probably cyclic within the upper slope of the Great Australian Bight, based on data presented in Holbourn et al. (in press). However, cyclicity cannot be proven without better chronostratigraphic control. Based upon much work done by many investigators (e.g., Chapell and Shackleton, 1986), orbital forcing of sea level cycles can be expected to be found in Pleistocene marine sediments that are neritic or are connected to a neritic source (i.e., periplatform—a shelf-slope linkage). However, predictable vertical lithologic, paleontologic, and diagenetic alternations will have to be demonstrated and tied to a stable-isotope chronostratigraphy, seismic stratigraphy, and the borehole logs to verify cyclicity.

If lithologic cyclicity is established and correlated to established astronomically tuned isotope curves, the facies architecture of the cycle can be tied to sea level changes. Thus, we can determine which sediments accumulate during the lowstand, rise, highstand, and fall and at what rates they accumulate during each phase of a sea level cycle.

QUESTIONS PRESENTED

So, are Milankovitch-scale lithologic cycles the basic stratigraphic building block of the Pleistocene sedimentary succession in the Great Australian Bight? If so, how are they constructed lithologically? When during a sea level cycle, how rapidly, and under what conditions did sediments accumulate? Do sediment facies change as sea level changes? Several other Leg 182 investigators are determining the possible presence of cycles and their facies architecture within the Pleistocene succession both at the eastern transect defined by Sites 1129, 1131, and 1127 (C. Betzler, pers. comm.), as well as the western transect defined by Sites 1132, 1130, and 1134 (Brooks et al., this volume).

To best answer these questions, an examination of the latest sea level events is required. We know sea level history probably within ± 10 -m elevation, since marine isotopic Stage (MIS) 5e or ~ 125 k.y. (e.g., Ku et al., 1974; Bard et al., 1990; Ludwig et al., 1996). Additionally, we know sea level behavior during the past 20 k.y. (or since the last glacial maximum [LGM]) better than any period of geologic time (e.g., Fairbanks, 1989; Locker et al., 1996; Bard et al., 1996; Fleming et al., 1998). Using the precision and small-sample requirements of ^{14}C accelerator mass spectrometry (AMS) dating, we can directly relate sediments to sea level

lowstand, transgression, and highstand. Since the present-day highstand is an ongoing event, the last sea level cycle is unfinished and is represented as Sequence 1 in Feary and James (1998). By defining the facies architecture of this unfinished cycle, we can more appropriately interpret the facies architecture of the earlier cycles embedded deeper in the Pleistocene succession.

We decided to concentrate on Site 1130 located in 488 m of water and the mid-depth site of the western transect. Site 1134, the deepest site, at 701 m, of the western transect, is actually located ~30 km to the west and out of the plane of Sites 1130 and 1132, which are directly up-dip/down-dip of each other (Fig. F1). Even though the eastern transect displayed a spectacular suite of prograding clinofolds built as a result of the highest sediment accumulation rates in the Great Australian Bight, we considered the western transect to be a more typical slope setting based on the work presented in Feary and James (1998). The stratal surfaces contained within the succession at the western transect are less progradation and more aggradational in geometry than those within the eastern transect which are decidedly progradational.

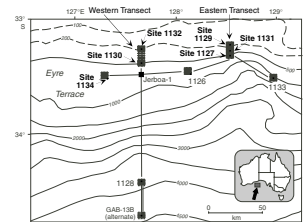
Additionally, we chose Site 1130 as a site of emphasis because it had not supported the bryozoan bioherms or bryozoan reef mounds as described by James et al. (2000). We purposely avoided the mounded seismic facies and concentrated on the parallel seismic stratal surfaces, because we were primarily interested in the results of transport processes moving sediments downslope from the upper slope bryozoan reef mounds or from the shelf itself. However, we conducted analyses on the thin (~7–10 m) post-LGM sedimentary cover overlying the now-buried mounds at sites in both the western and eastern transects. James et al. (2000) demonstrated that the bryozoan reef mounds were active during and prior to the LGM and ceased growing after the LGM. The nature of this cover or drape overlying these mounds will provide us with information on sediment accumulation during the transgressive/highstand phase of the sea level cycle, since James et al. (2000) demonstrated that the bryozoan mounds are lowstand features.

METHODS

AMS ¹⁴C Dating

Sediment samples were submitted to the National Ocean Sciences AMS Facility (NOSAMS) at the Woods Hole Oceanographic Institution (Table T1). To determine if there was a difference in source area and a potential age difference between the fine and coarse fraction, grain size splits were made. Separate dates from the fine fraction (<63 μm), total bulk sediment, and bulk sand-sized fraction were obtained. AMS dates were calculated using 5568 yr as a half-life of radiocarbon and are presented without reservoir corrections or calibration to calendar years. Radiocarbon dates provided by A. Holbourn (pers. comm.) were obtained from benthic foraminifers, and those dates provided by James et al. (2000) were obtained from species-specific bryozoans (*Celleporaria* sp.). Sediment accumulation rates were calculated using dates from the <63-μm bulk sediment fraction, the bulk sand fraction, and the bulk sediment fraction (Table T2).

F1. Location map of Leg 182 sites, p. 10.



T1. Radiocarbon AMS dating results, p. 17.

T2. Calculated sedimentation accumulation rates, p. 18.

Sedimentology and Geochemistry

Based upon the radiocarbon dating, 20-cm³ samples at ~1 m intervals were obtained from the upper 20 meters below seafloor (mbsf) or less from Sites 1132, 1130, and 1134 (western transect) (Figs. F2, F3, F4; Tables T3, T4, T5) and from Sites 1129, 1131, and 1128 (eastern transect) (Figs. F5, F6, F7; Tables T5, T6, T7). Grain size distributions were measured for the coarse fraction (>63 μm) using the settling tube method (Gibbs, 1974) and for the fine fraction (<63 μm) using the pipette method (Folk, 1965).

Acid leaching (Milliman, 1974) was used to determine calcium carbonate content.

Using the insoluble residue from the calcium carbonate analysis, total organic carbon content was determined through the loss on ignition (LOI) method (Dean, 1974). Approximately 1 g of sample residue (weighed to four decimal places in a crucible of known weight) was placed in a 550°C furnace for 4 hr, cooled, and reweighed. Resulting weights from the before and after difference were entered into an equation that related to the original sample before calcium carbonate analysis.

Carbonate mineralogy was determined through powder X-ray diffraction (XRD) using a Scintag XDS 2000 θ/θ goniometer with a 2.2-kW sealed copper X-ray source. Bulk carbonate analyses were performed on all samples, which were ground and prepared using the glass slide method and dried at room temperature (Moore and Reynolds, 1997). Quantitative carbonate mineralogy was determined using a calibration of the ratio of aragonite, dolomite, and high-Mg calcite (HMC) to the sum of low-Mg calcite (LMC) and HMC. See Swart et al. (this volume) for additional details.

RESULTS

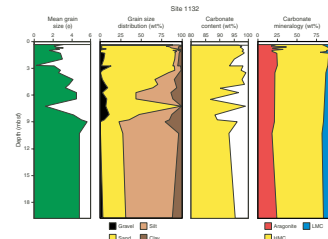
AMS ¹⁴C Dating

Western Transect

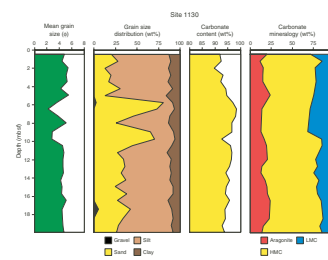
Site 1132 is the shallowest site (Hole B, 218.5 m) in the western transect and supports mounded features (Holbourn et al., in press). The two older dates (26.45 and 36.77 ka) are from benthic foraminifers and are contemporaneous with the bryozoan mound growth, indicating a sediment accumulation rate of 76 cm/k.y. (Tables T1, T2). At 2.3 mbsf, a 21.50-ka date from total bulk sediment was obtained indicating a sediment accumulation rate of 11 cm/k.y. from this point in time until the present. These calculations indicate a reduction of sediment accumulation rate at this site by seven times since the byrozoan mounds were terminated at MIS 2 (James et al., 2000). The sediments in the upper 20 m of this site are alternating white, light gray, and pale yellow bryozoan floatstones, grainstones, and packstones—all heavily bioturbated. The allochems are mostly broken debris of delicate and robust branching bryozoans and benthic foraminifers. The matrix consists of nannofossils, foraminifers, and sponge and tunicate spicules. All sediment descriptions are from Feary, Hine, Malone, et al. (2000).

A total of 12 AMS dates were obtained from Site 1130 (Hole 1130A), located in 486.7 m of water downslope of the buried bryozoan mounds at Site 1132 (Table T1). AMS dates from the <63-μm fraction,

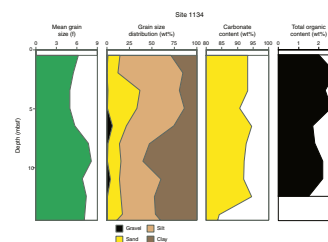
F2. Grain size, carbonate content, and mineralogy, Site 1132, p. 11.



F3. Grain size, carbonate content, and mineralogy, Site 1130, p. 12.



F4. Grain size, carbonate content, and total organic carbon, Site 1134, p. 13.



T3. Grain size and mineralogical data, Site 1132, p. 19.

T4. Grain size and mineralogical data, Site 1130, p. 20.

T5. Grain size, carbonate, and total organic carbon data, Site 1134, p. 21.

the sand fraction, and total bulk sediment were obtained. The <63- μm fraction dates were always younger than the dates obtained from the bulk sand fraction. At 5.73 mbsf, dates were obtained from the <63- μm fraction (19.0 ka), bulk sand fraction (27.6 ka), and total bulk sediment (24.5 ka). This was the only location where dates were obtained from these three different grain size fractions. The total bulk sediment date fell between the dates obtained from the <63- μm fraction and the bulk sand fraction. The dominant sediment is a moderately to heavily bioturbated pale olive and light gray bioclastic packstone. The coarse fraction is dominantly unidentifiable skeletal debris, benthic foraminifers, and sponge spicules. The matrix consists of nannofossils, tunicate and sponge spicules, small quartz grains, and minor clay.

Various sediment accumulation rates were calculated based upon the grain size of the material dated (Table T2). These rates varied over a wide range of values for similar, but not exactly the same, periods of time, indicating that different sediment sources, different transport mechanisms, and bioturbation were involved and active. However, these dates generally show that sediment accumulation rates decreased toward the top of the succession.

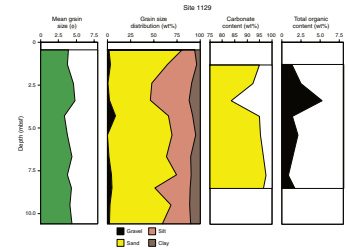
Site 1134 (Hole 1134A), in the deepest water on this transect (701.0 m), provided a 38.1-ka date at the uppermost sample (1.95 mbsf). Extending down to 10.95 mbsf, a date of 44.2 ka was obtained making the age difference of this section 6.1 ka. Note that there is stratigraphic inversion within the dates at this site. All dates were from <63- μm bulk sediment. The sediment accumulation rate from the youngest date obtained at this site to present is 5 cm/k.y., making it the lowest of all calculated in this study. The dominant sediments are alternating light gray, light olive gray, and white nannofossil oozes with planktonic foraminifer and bioclasts. These sediments are texturally wackestone and are moderately to heavily bioturbated.

Eastern Transect

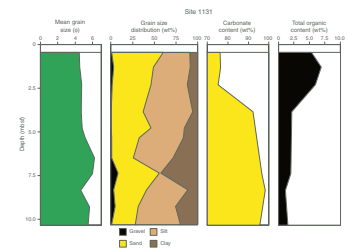
Site 1131 (Hole 1131A in 333.6 m water depth; Hole 1131B in 331.4 m water depth) is the intermediate site of a three-site depth transect termed the eastern transect. No data were obtained from Site 1129, the shallowest site along the eastern transect, because of the proximity of the bryozoan reef mounds in the shallow subsurface. James et al. (2000) point out that the bryozoan reef mounds were active no later than 26.61 k.y. at 11.2 mbsf and were covered by a 7- to 10-m-thick drape that lacks the prolific bryozoans found in the mounds beneath. This drape is a massive, homogenous, light gray, unlithified bioclastic packstone. The bryozoan reef mounds below are texturally floatstone (James et al., 2000). AMS dates from this drape were obtained from both the <63- μm bulk sediment and from the bulk sand fraction.

Hole 1127B was the deepest hole along the eastern transect lying in 479.3 m of water. There were no bryozoan reef mounds encountered here. The uppermost 6 m of the section consisted of a nannofossil ooze overlying a foraminiferal ooze. Below 6 mbsf, a thick section of alternating bioclastic wackestone- and packstone-dominated packages were predominant. Radiocarbon AMS dates reveal that the <63- μm bulk sediment fraction provided dates that were younger or the same as age as dates from the bulk sand fraction (Table T1). Calculated accumulation rates from the <63- μm bulk sediment fraction and the bulk sand fraction are similar except that the oldest date from the bulk sand fraction is stratigraphically inverted and contrasts sharply with the

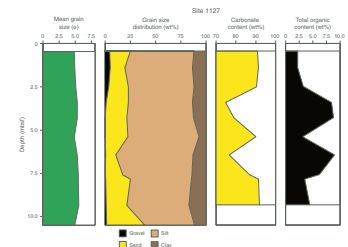
F5. Grain size, carbonate content, and organic carbon, Site 1129, p. 14.



F6. Grain size, carbonate content, and organic carbon, Site 1131, p. 15.



F7. Grain size, carbonate content, and organic carbon, Site 1127, p. 16.



T6. Grain size, carbonate, and total organic carbon, Site 1129, p. 22.

T7. Grain size, carbonate, and total organic carbon, Site 1131, p. 23.

275 cm/k.y. rate calculated from the two older dates obtained from the <63- μ m bulk sediment fraction (Table T2).

Sedimentology and Geochemistry

Western Transect

Site 1132 grain size data indicate a coarsening upward trend from ~9 mbsf as a result of increased gravel- and sand-sized fractions (Fig. F2; Table T3). At 7.25 mbsf there is a pronounced increase in coarser material. This location within the hole corresponds approximately to the top of the bryozoan reef mounds. There is another coarser unit at 2.7 mbsf. Carbonate content is quite variable over the top 9-m-long section displayed with values ranging from 86.7 to 98.4 wt%. Carbonate mineralogy is mostly invariant with HMC being dominant extending down to the bottom of the section examined here at 19.8 mbsf.

Grain size data at Site 1130 reveals two pronounced sand-dominated units at 5.73 and 9.73 mbsf (Fig. F3; Table T4). Both of these occur approximately within the time frame bracketed by the 19.00- to 26.90-ka AMS dates from the <63- μ m bulk sediment fraction (Table T1). These dates lie within MIS 2 and the last glacial maximum. The sediments are dominantly HMC, but there is an overall increase in LMC as compared to Site 1132.

Grain size at Site 1134 is much finer grained although both gravel- and sand-sized sediments are found (Fig. F4; Table T5). The 14.45 mbsf section examined has a coarser-grained upper unit and a finer grained lower unit, with the transition occurring at ~6 mbsf. Carbonate content is generally between 90 and 95 wt% but drops to below 84 wt% at the bottom of the section examined at this site.

Eastern Transect

The upper 10 mbsf at Site 1129 is sand dominated with some gravel (Fig. F5; Table T6). Sand increases in content within the uppermost 2.5 m of this section. Where there is a noticeable drop in carbonate content, there is a corresponding increase in total organic content. At some point below this studied section lie the bryozoan reef mounds.

At Site 1131 there is also an increase in sand from ~10.36 mbsf, the base of this studied section, to the top (Fig. F6; Table T7). This encompasses almost all of the sedimentary cover or drape that lies on top of the buried bryozoan reef mounds, which are encountered at ~11.2 mbsf. Note the same relationship between carbonate content and total organic carbon as seen at Site 1129. Overall, the sediments here at Site 1131 are finer grained than those at the shallower Site 1129.

At Site 1127, the deepest site along the eastern transect, this sedimentary section is finer grained than both those sections examined at Site 1129 and Site 1131 (Fig. F7; Table T8). Grain size trends are less variant. Again, there is an inverse relationship between carbonate content and total organic carbon.

T8. Grain size, carbonate, and total organic carbon, Site 1127, p. 24.

ACKNOWLEDGMENTS

We thank our fellow members of the Leg 182 Shipboard Party and the ODP staff who sailed with us, particularly Staff Scientist Dr. Mitchell J. Malone. We greatly appreciate the hard work of the crew of the

JOIDES Resolution, sometimes under frustrating and dangerous conditions. We thank the ODP shore-based staff at Texas A&M University, particularly those in publications and curation. We acknowledge support from the U.S. National Science Foundation (NSF) for supporting the NOSAMS Facility through National Science Foundation Cooperative Agreement OCE-9807266. This research used samples provided by ODP. ODP is sponsored by the NSF and participating countries under management of Joint Oceanographic Institutions (JOI), Inc. Funding for this research was provided by a grant from JOI-USSSP. We thank Drs. Benjamin Flower and Pamela Hallock, College of Marine Science, University of South Florida, for their advice and expertise.

REFERENCES

- Bard, E., Hamelin, B., Arnold, M., Montaggioni, L.F., Cabioch, G., Faure, G., and Rougerie, F., 1996. Deglacial sea level record from Tahiti corals and the timing of global meltwater discharge. *Nature*, 382: 241–244.
- Bard, E., Hamelin, B., and Fairbanks, R.G., 1990. U-Th ages obtained by mass spectrometry in corals from Barbados: sea level during the past 130,000 years. *Nature*, 346:456–458.
- Chapell, J., and Shackleton, N.J., 1986. Oxygen isotopes and sea level. *Nature*, 324:137–140.
- Dean, W.E., 1974. Determination of carbonate and organic matter in calcareous sediments and sedimentary rocks by loss on ignition. *J. Sediment. Petrol.*, 44:242–248.
- Eberli, G.P., Swart, P.K., Malone, M.J., et al., 1997. *Proc. ODP, Init. Repts.*, 166: College Station, TX (Ocean Drilling Program).
- Fairbanks, R.G., 1989. A 17,000-year glacio-eustatic sea level record: influence of glacial melting rates on the Younger Dryas event and deep-ocean circulation. *Nature*, 342:637–642.
- Feary, D.A., Hine, A.C., Malone, M.J., et al., 2000. *Proc. ODP, Init. Repts.*, 182 [CD-ROM]. Available from: Ocean Drilling Program, Texas A&M University, College Station, TX 77845-9547, U.S.A.
- Feary, D.A., and James, N.P., 1998. Seismic stratigraphy and geological evolution of the Cenozoic, cool-water, Eucla Platform, Great Australian Bight. *AAPG Bull.*, 82:792–816.
- Fleming, K., Johnston, P., Zwartz, D., Yoyoyama, Y., Lambeck, K., and Chapell, J., 1998. Refining the eustatic sea-level curve since the “Last Glacial Maximum” using far- and intermediate-field sites. *Earth Planet. Sci. Lett.*, 163:327–342.
- Folk, R.L., 1965. *Petrology of Sedimentary Rocks*: Austin, TX (Hemphill’s).
- Gibbs, R.J., 1974. A settling tube for sand-sized analysis. *J. Sediment. Petrol.*, 44:583–588.
- Glaser, K.S., Droxler, A.W., and Baker, P.A., 1991. Highstand shedding off two semi-drowned shallow carbonate systems, Pedro Bank and the southern shelf of Jamaica, northeastern Nicaraguan Rise. *J. Sediment. Petrol.*, 61:128–142.
- Holbourn, A., Kuhnt, W., and James, N.P., in press, Late Pleistocene isotope stratigraphy and paleoceanography of the Great Australian Bight: the benthic foraminiferal record. *Paleoceanography*.
- Imbrie, J., Hays, J.D., Martinson, D.G., McIntyre, A., Mix, A.C., Morley, J.J., Pisias, N.G., Prell, W.L., and Shackleton, N.J., 1984. The orbital theory of Pleistocene climate: support from a revised chronology of the marine $\delta^{18}\text{O}$ record. In Berger, A., Imbrie, J., Hays, J., Kukla, G., and Saltzman, B. (Eds.), *Milankovitch and Climate* (Pt. 1), NATO ASI Ser. C, Math Phys. Sci., 126:269–305.
- James, N.P., 1997. The cool-water carbonate depositional realm. In James, N.P. and Clarke, J.A.D (Eds.), *Cool-Water Carbonates*. Spec. Publ.—SEPM (Soc. Sediment. Geol.), 56:1–20.
- James, N.P., Feary, D.A., Surlyk, F., Simo, J.A., Betzler, C., Holbourn, A.E., Li, Q., Matsuda, H., Machiyama, H., Brooks, G.R., Andres, M.S., Hine, A.C., Malone, M.J., and the ODP Leg 182 Science Party, 2000. Quaternary bryozoan reef mounds in cool-water, upper slope environments, Great Australian Bight. *Geology*, 28:647–650.
- Ku, T.L., Kimmel, M.A., Easton, W.H., and O’Neil, T.J., 1974. Eustatic sea level 120,000 years ago on Oahu, Hawaii. *Science*, 183:959–962.
- Locker, S.D., Hine, A.C., Tedesco, L.P., and Shinn, E.A., 1996. Magnitude and timing of episodic sea-level rise during the last deglaciation. *Geology*, 24:827–830.
- Ludwig, K.R., Muhs, D.R., Simmons, K.R., Halley, R.B., and Shinn, E.A., 1996. Sea-level records at ~80 ka from tectonically stable platforms: Florida and Bermuda. *Geology*, 24:211–214.

- Martinson, D.G., Pisias, N.G., Hays, J.D., Imbrie, J., Moore, T.C., Jr., and Shackleton, N.J., 1987. Age dating and the orbital theory of the ice ages: development of a high-resolution 0 to 300,000-year chronostratigraphy. *Quat. Res.*, 27:1–29.
- Milliman, J.D., 1974. *Marine Carbonates* (2nd ed.): Berlin (Springer-Verlag).
- Moore, D.M. and Reynolds, R.C., 1997. *X-Ray Diffraction and the Identification and Analysis of Clay Minerals* (2nd edition): Oxford (Oxford Univ. Press).
- Mullins, H.T., Gardulski, A.F., Hinchey, E.J., and Hine, A.C., 1988a. The modern carbonate ramp slope of central west Florida: *J. Sediment. Petrol.*, 58:273–290.
- Mullins, H.T., Gardulski, A.F., Hine, A.C., Melillo, A.J., Wise, S.W., Jr., and Applegate, J., 1988b. Three-dimensional sedimentary framework of the carbonate ramp slope of central west Florida: a sequential seismic stratigraphic perspective. *Geol. Soc. Am. Bull.*, 100:514–533.

Figure F1. Location map of Leg 182 sites, including the western and eastern transects.

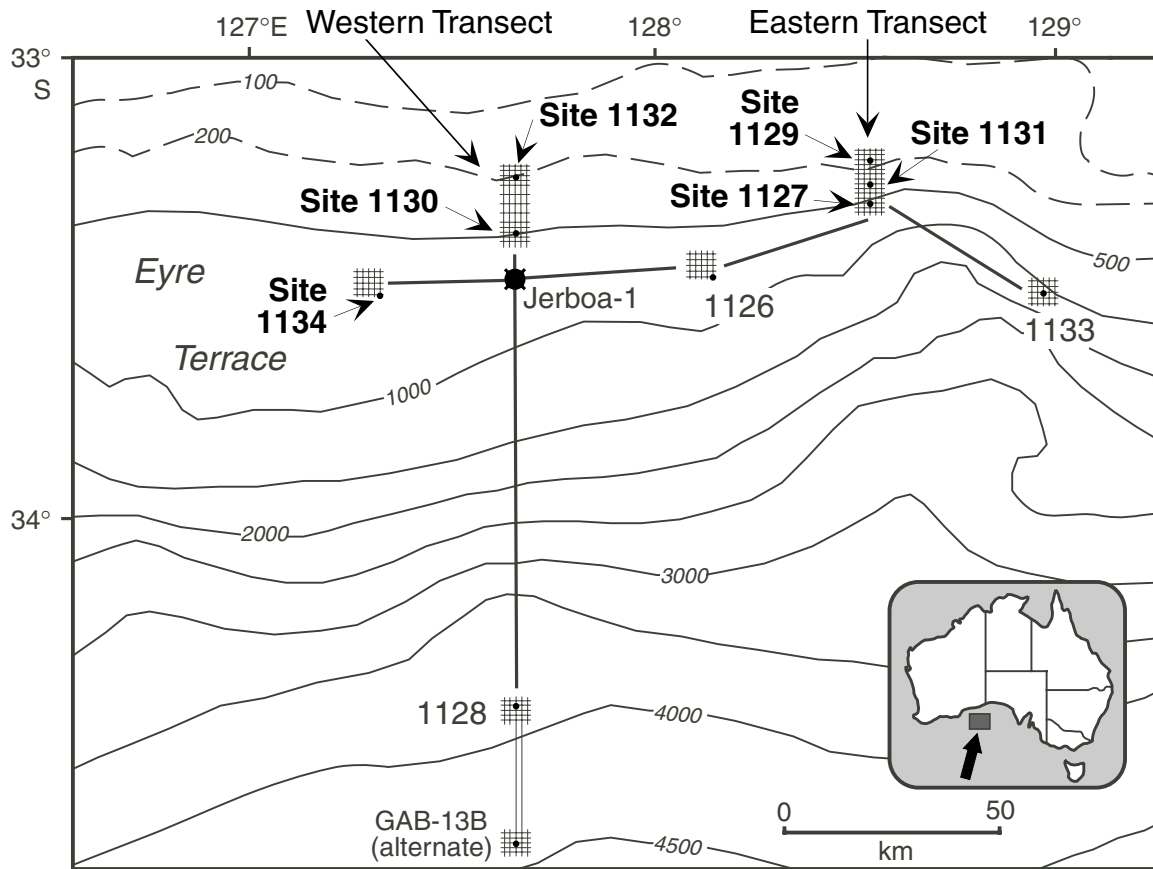


Figure F2. Grain size, carbonate content, and mineralogy data, Site 1132. HMC = high-Mg calcite, LMG = low-Mg calcite.

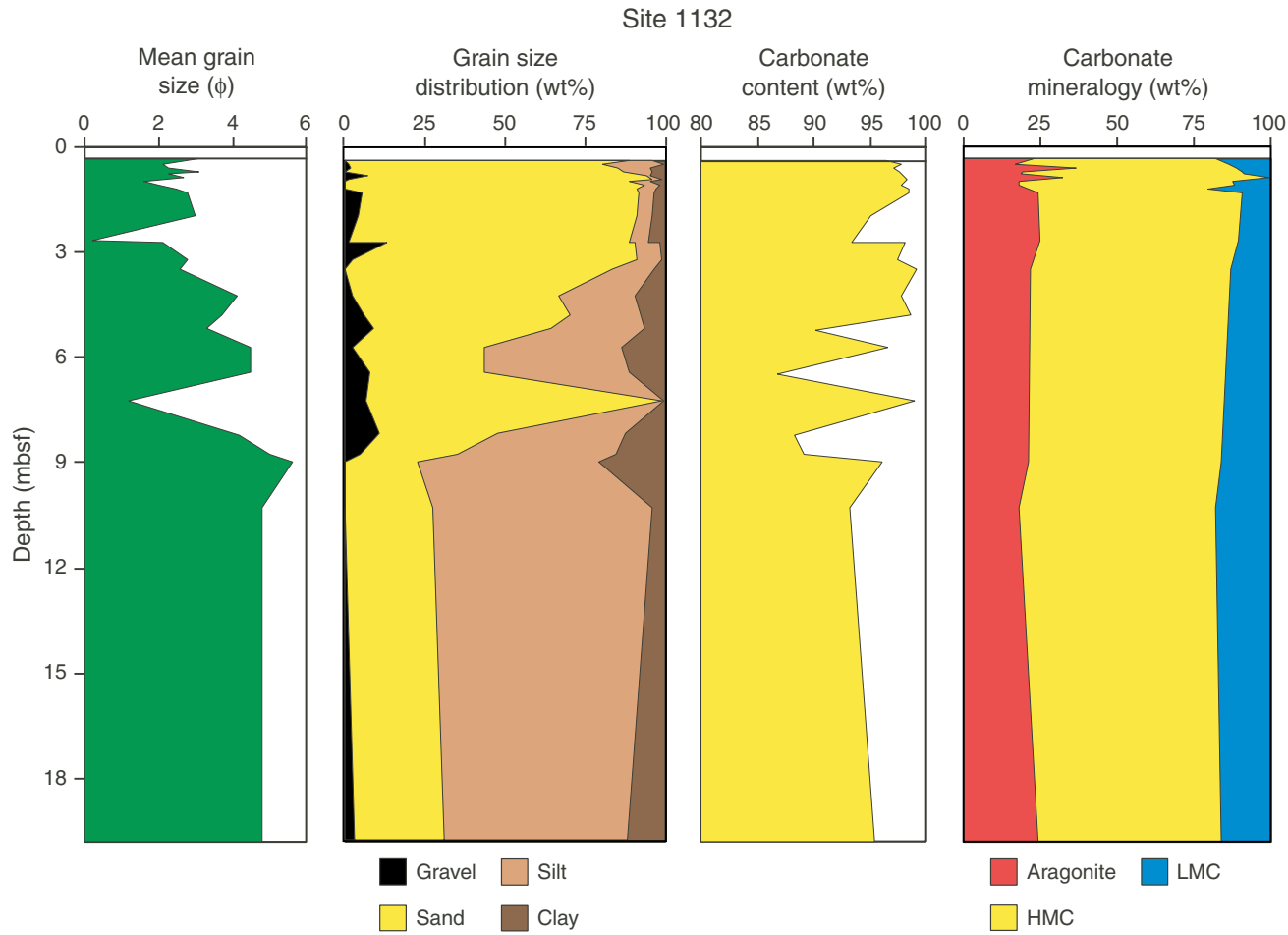


Figure F3. Grain size, carbonate content, and mineralogy data, Site 1130. HMC = high-Mg calcite, LMG = low-Mg calcite.

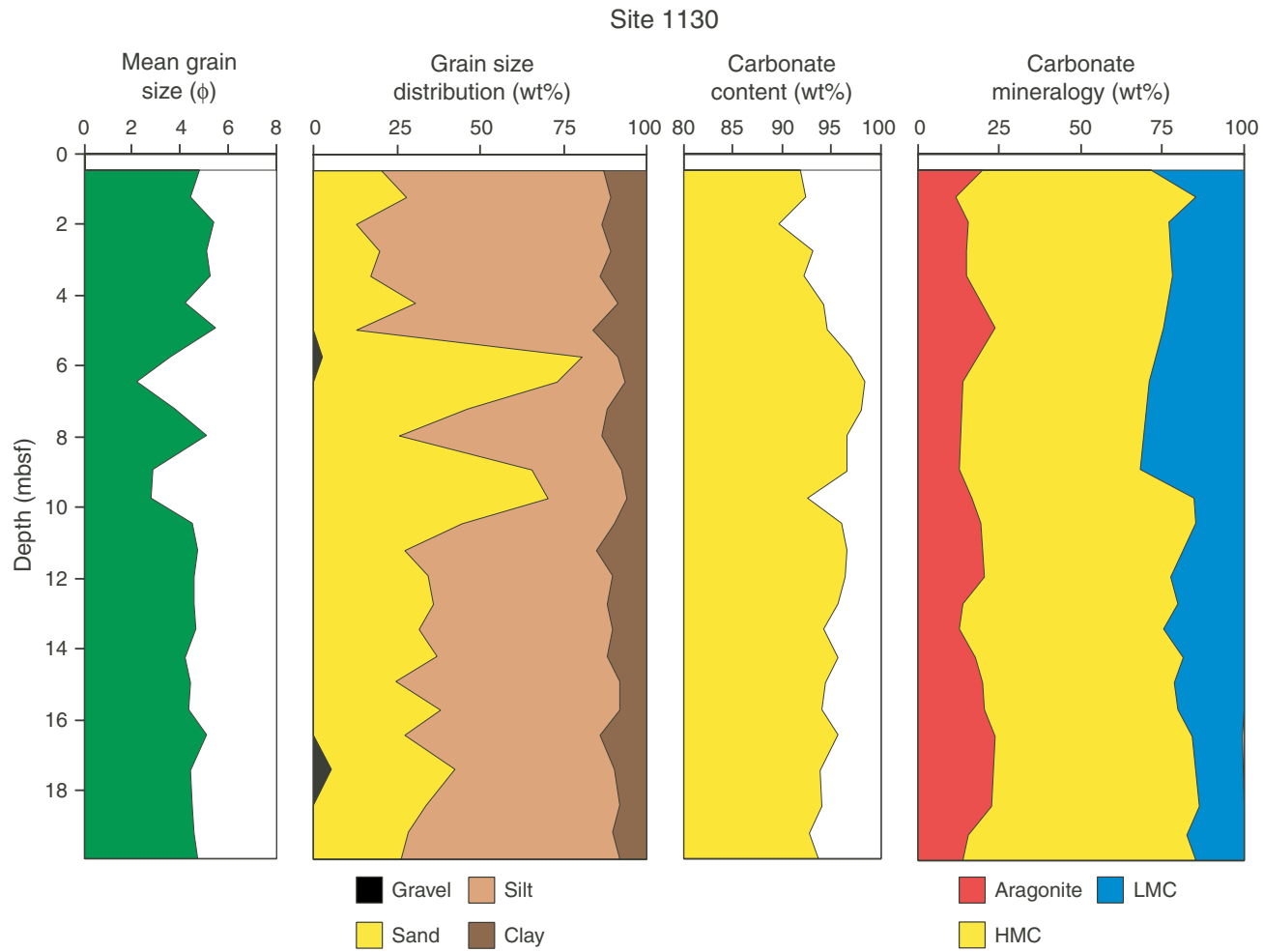


Figure F4. Grain size, carbonate content, and total organic carbon data, Site 1134.

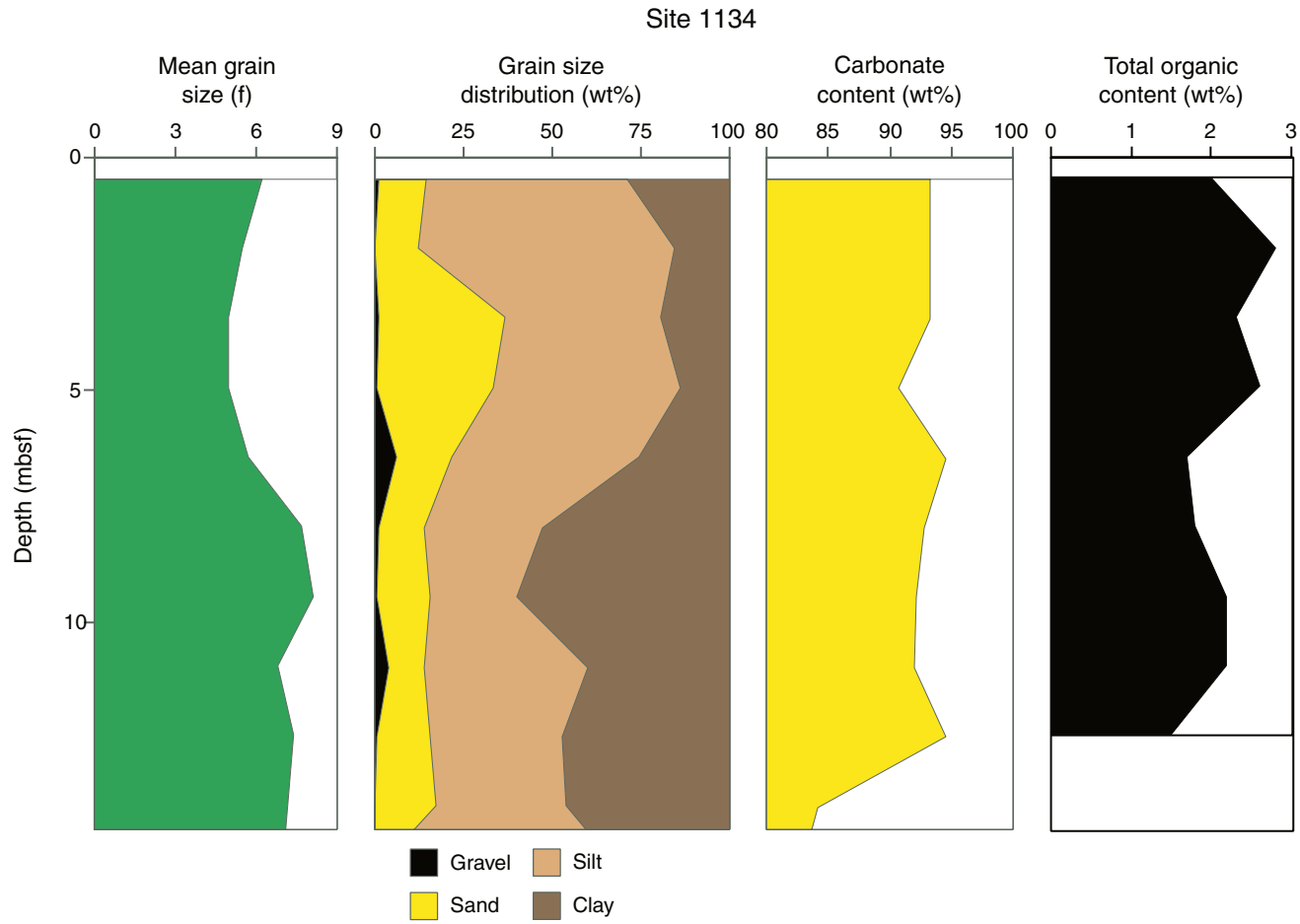


Figure F6. Grain size, carbonate content, and total organic carbon data, Site 1131.

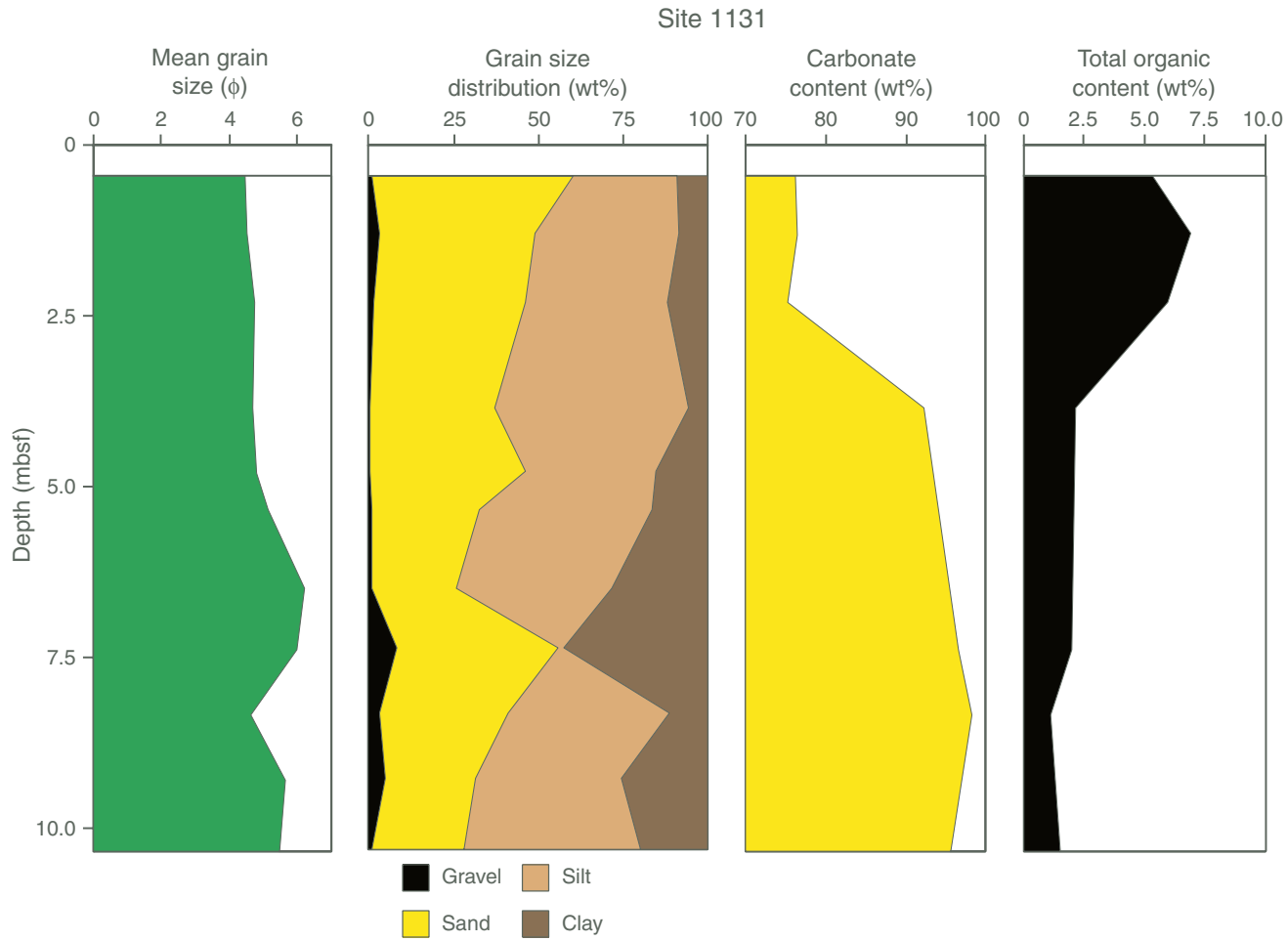


Figure F7. Grain size, carbonate content, and total organic carbon data, Site 1127.

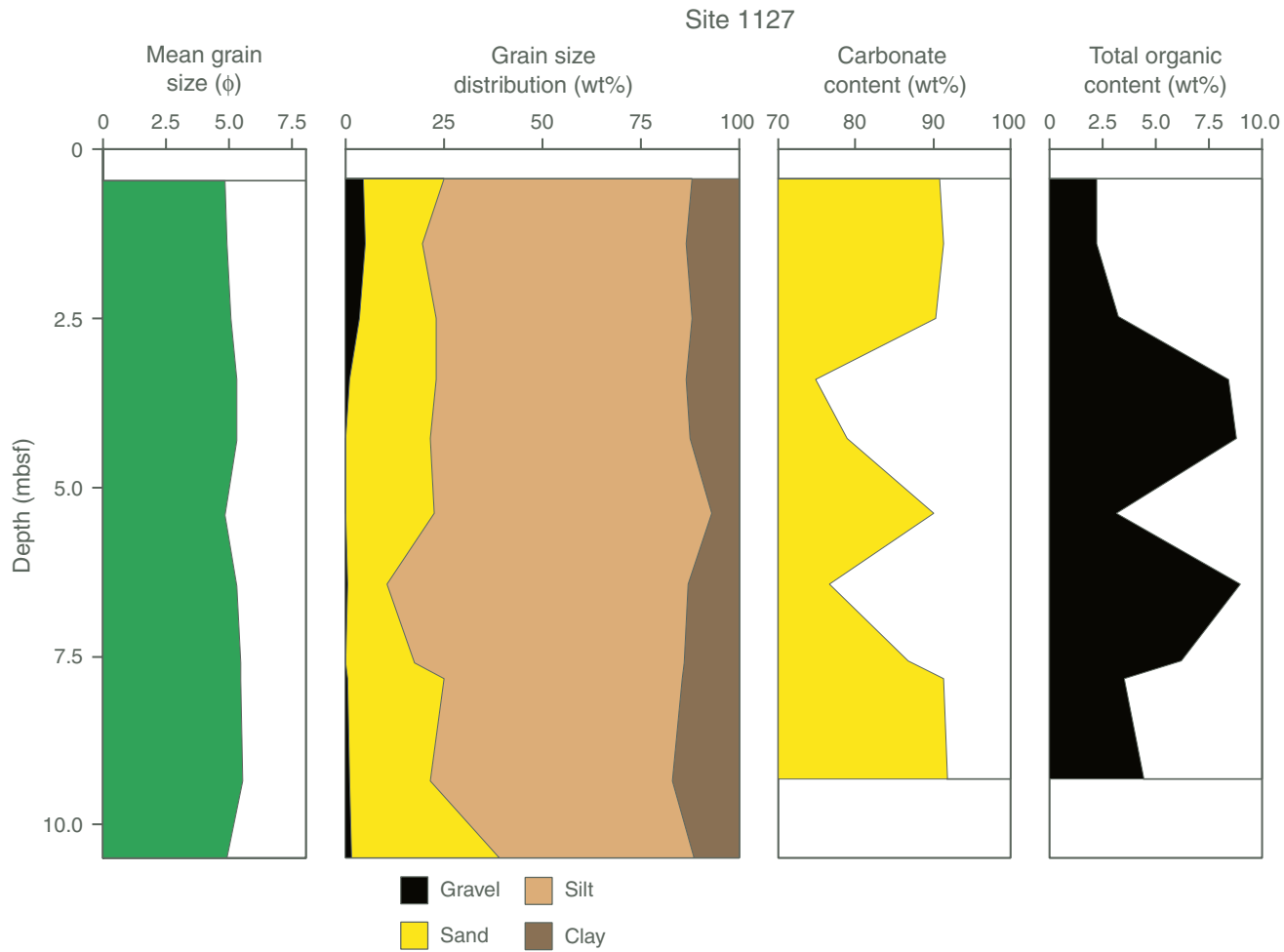


Table T1. Radiocarbon AMS dating results.

Core, section, interval (cm)	Depth (mbsf)	Date (ka)	Sample type
Western Transect (shallow to deep)			
182-1132B-	2.3	21.50 ± 0.110	Total bulk sediment
1H-2, 70–72	6.7	26.45 ± 0.220	Benthic foraminifers
1H, CC*	14.53	36.77 ± 0.660	Benthic foraminifers
2H-6, 23–28*			
182-1130A-	2.73	13.30 ± 0.085	<63 µm, bulk sediment
1H-2, 123–125	2.73	13.55 ± 0.150	Total bulk sediment
1H-2, 123–125	4.96	13.95 ± 0.055	<63 µm, bulk sediment
1H-4, 45–47	4.96	17.45 ± 0.120	Bulk sand fraction
1H-4, 45–47	5.73	19.00 ± 0.150	<63 µm, bulk sediment
1H-4, 123–125	5.73	27.60 ± 0.150	Bulk sand fraction
1H-4, 123–125	5.73	24.50 ± 0.300	Total bulk sediment
1H-4, 123–125	7.96	27.40 ± 0.150	<63 µm, bulk sediment
1H-6, 45–47	7.96	29.70 ± 0.200	Bulk sand fraction
1H-6, 45–47	10.45	26.90 ± 0.190	<63 µm, bulk sediment
2H-2, 45–47	10.45	27.70 ± 0.360	Total bulk sediment
2H-2, 45–47	16.47	38.39 ± 0.390	Total bulk sediment
2H-6, 45–47			
182-1134A-	1.95	38.10 ± 0.360	<63 µm, bulk sediment
1H-2, 45–47	4.95	41.50 ± 0.480	<63 µm, bulk sediment
2H-1, 45–47	7.95	39.70 ± 0.460	<63 µm, bulk sediment
2H-3, 45–47	10.95	44.20 ± 550	<63 µm, bulk sediment
2H-5, 45–47			
Eastern transect (shallow to deep)			
182-1131A-			
1H-1, 45–49	0.48	2.65 ± 0.035	<63 µm, bulk sediment
1H-1, 45–49	0.48	5.26 ± 0.045	Bulk sand fraction
2H-1, 140–144	4.82	15.40 ± 0.090	<63 µm, bulk sediment
2H-1, 140–144	4.82	14.05 ± 0.060	Bulk sand fraction
2H-3, 10–4	6.52	17.40 ± 0.080	<63 µm, bulk sediment
2H-3, 10–14	6.52	16.75 ± 0.100	Bulk sand fraction
182-1131B-			
2H-2, 140–145†	11.2	26.61 ± 0.190	Bryozoans
2H-4, 97–100†	13.8	34.62 ± 0.490	Bryozoans
2H-5, 5–10†	14.4	35.12 ± 0.520	Bryozoans
182-1127B-			
1H-1, 45–49	0.48	3.68 ± 0.040	<63 µm, bulk sediment
1H-1, 45–49	0.48	4.45 ± 0.055	Bulk sand fraction
1H-3, 130–134	4.32	11.40 ± 0.045	<63 µm, bulk sediment
1H-3, 130–134	4.32	13.95 ± 0.050	Bulk sand fraction
2H-1, 47–51	7.49	12.55 ± 0.045	<63 µm, bulk sediment
2H-1, 47–51	7.49	12.55 ± 0.085	Bulk sand fraction

Notes: AMS = auxiliary measuring sonde. * = A. Holbourn (pers. comm.). † = James et al., 2000.

Table T2. Calculated sedimentation accumulation rates based on radiocarbon AMS dates.

Time frame (ka)	Depth range (mbsf)	Accumulation rate (cm/k.y.)
Western transect		
182-1132B-		
Dates from bulk sediment and benthic foraminifers		
0–21.50	0–2.3	11
21.50–26.45	2.3–6.7	89
26.45–36.77	66.7–14.53	76
182-1130A-		
Dates from <63- μ m bulk sediment fraction		
0–13.30	0–2.73	21
13.30–13.95	2.73–4.96	343
13.95–19.00	4.96–5.73	656
19.00–27.40	5.73–7.96	27
27.40–26.90	7.96–10.45	Stratigraphically inverted
Dates from bulk sand fraction		
0–17.45	0–4.96	28
17.45–27.60	4.96–5.73	7.5
27.60–29.70	5.73–7.96	106
Dates from bulk sediment (<63- μ m and sand fractions combined)		
0–13.55	0–2.73	20
13.55–24.50	2.73–5.73	27
24.50–27.70	5.73–10.45	148
27.70–38.39	10.45–16.47	56
182-1134A-		
0–38.10	0–1.95	5
38.10–44.20	1.95–10.95	148
Eastern transect		
182-1131A-		
Dates from <63- μ m bulk sediment fraction		
0–2.65	0–0.48	18
2.65–15.40	0.48–4.82	34
15.40–17.40	4.82–6.52	85
Dates from bulk sand fraction		
0–5.26	0–0.48	9
5.26–14.05	0.48–4.82	49
14.05–16.75	4.82–6.52	63
182-1131B-		
Dates from <i>Celleporaria</i> sp. bryozoan		
26.61–34.62	11.2–13.8	32
34.62–35.12	13.8–14.4	12
Site 1127B		
Dates from <63- μ m bulk sediment fraction		
0–3.68	0–0.48	13
3.68–11.40	0.48–4.32	49
11.40–12.55	4.32–7.29	275
Dates from bulk sand fraction		
0–4.45	0–0.48	11
4.45–13.95	0.48–4.32	40
13.95–12.55	4.32–7.28	Stratigraphically inverted

Note: AMS = auxiliary measuring sonde.

Table T3. Grain size and mineralogical data, Site 1132.

Core, section, interval (cm)	Depth (mbsf)	Mean (φ)	Gravel (wt%)	Sand (wt%)	Silt (wt%)	Clay (wt%)	Carbonate (wt%)	Aragonite (wt%)	HMC (wt%)	LMC (wt%)	Dolomite (wt%)
182-1132B-											
1H-1, 36–38	0.36	3.1	0.0	88.9	7.3	3.8	96.4	22.9	59.6	17.5	0.0
1H-1, 50–52	0.50	2.1	1.0	79.9	19.2	0.0	97.7	16.9	69.9	13.2	0.0
1H-1, 60–62	0.60	2.3	1.6	83.8	10.5	4.1	97.1	36.5	52.8	10.7	0.0
1H-1, 70–72	0.70	3.1	0.0	87.3	8.9	3.9	97.6	19.1	72.4	8.6	0.0
1H-1, 80–82	0.80	2.3	7.1	87.4	1.4	4.2	97.9	18.3	73.5	8.2	0.0
1H-1, 90–92	0.90	2.7	1.1	94.9	3.2	0.8	98.3	32.6	67.4	0.1	0.0
1H-1, 100–102	1.00	1.6	0.0	89.2	6.7	4.1	98.1	18.0	70.2	11.8	0.0
1H-1, 110–112	1.10	2.0	0.0	93.8	4.7	1.5	97.8	17.7	71.2	11.1	0.0
1H-1, 120–122	1.20	2.5	0.0	91.6	5.9	2.5	98.4	20.7	59.4	19.9	0.0
1H-1, 130–132	1.30	2.8	5.1	86.8	5.1	3.1	98.4	24.3	67.0	8.4	0.2
1H-2, 45–47	1.95	3.0	4.2	87.2	4.7	3.9	95.1	ND	ND	ND	ND
1H-2, 70–72	2.70	0.2	0.9	88.4	5.5	5.1	93.4	24.6	65.4	10.0	0.0
1H-2, 123–125	2.73	2.1	13.1	77.7	7.8	1.4	98.1	ND	ND	ND	ND
1H-3, 20–22	3.20	2.8	2.3	89.1	7.8	0.8	97.5	ND	ND	ND	ND
1H-3, 50–52	3.50	2.6	0.0	83.9	12.9	3.1	99.1	21.4	65.8	12.8	0.0
1H-3, 123–125	4.23	4.1	2.0	64.7	23.9	9.4	97.7	ND	ND	ND	ND
1H-4, 30–32	4.80	3.7	5.6	64.9	22.4	7.1	98.6	ND	ND	ND	ND
1H-4, 70–72	5.20	3.3	8.6	55.6	29.6	6.2	90.2	ND	ND	ND	ND
1H-4, 123–125	5.73	4.5	2.3	41.0	43.2	13.5	96.6	ND	ND	ND	ND
1H-5, 45–47	6.45	4.5	7.4	36.3	45.2	11.1	86.7	ND	ND	ND	ND
2H-1, 45–47	7.25	1.2	6.2	93.3	0.5	0.0	99.0	ND	ND	ND	ND
2H-1, 140–142	8.20	4.2	10.4	37.6	39.7	12.4	88.3	ND	ND	ND	ND
2H-2, 45–47	8.75	5.0	4.8	30.1	49.9	15.2	89.1	ND	ND	ND	ND
2H-2, 70–72	9.00	5.6	0.0	22.4	57.1	20.5	96.1	20.9	63.2	16.0	0.0
2H-3, 50–52	10.30	4.8	0.0	27.3	69.0	3.7	93.2	18.1	64.6	17.2	0.0
3H-3, 50–52	19.80	4.8	2.7	28.0	57.6	11.7	95.4	24.2	60.1	15.7	0.0

Notes: ND = no data. HMC = high-Mg calcite, LMC = low-Mg calcite.

Table T4. Grain size and mineralogical data, Site 1130.

Core, section, interval (cm)	Depth (mbsf)	Mean (ϕ)	Gravel (wt%)	Sand (wt%)	Silt (wt%)	Clay (wt%)	Carbonate (wt%)	Aragonite (wt%)	HMC (wt%)	LMC (wt%)	Dolomite (wt%)
182-1130A-											
1H-1, 45-47	0.45	4.8	0.0	20.4	66.6	13.0	91.9	19.8	51.5	28.7	0.0
1H-1, 123-125	1.23	4.4	0.0	27.8	61.1	11.1	92.4	11.8	73.5	14.7	0.0
1H-2, 45-47	1.95	5.4	0.0	12.8	73.8	13.4	89.7	15.5	61.7	22.9	0.0
1H-2, 123-125	2.73	5.1	0.0	19.9	69.3	10.8	93.1	15.0	62.8	22.3	0.0
1H-3, 45-47	3.45	5.2	0.0	17.2	68.4	14.4	92.3	14.8	63.6	21.6	0.0
1H-3, 123-125	4.23	4.2	0.0	30.3	60.9	8.8	94.2	ND	ND	ND	ND
1H-4, 45-47	4.95	5.5	0.0	13.1	70.5	16.5	94.7	23.7	51.8	24.6	0.0
1H-4, 123-125	5.73	3.6	2.4	78.0	10.6	9.0	97.0	ND	ND	ND	ND
1H-5, 45-47	6.45	2.2	0.0	73.0	20.5	6.5	98.4	13.7	57.3	29.0	0.0
1H-5, 123-125	7.23	3.7	0.0	46.0	41.8	12.2	98.0	ND	ND	ND	ND
1H-6, 45-47	7.95	5.1	0.0	25.9	60.3	13.8	96.5	ND	ND	ND	ND
2H-1, 45-47	8.95	2.9	0.0	65.7	26.4	7.9	96.5	13.0	55.5	31.5	0.0
2H-1, 123-125	9.73	2.8	0.0	70.0	23.6	6.3	92.6	16.7	67.8	15.5	0.0
2H-2, 45-47	10.45	4.5	0.0	44.3	45.7	10.0	96.0	19.2	65.9	14.9	0.0
2H-2, 123-125	11.23	4.7	0.0	27.6	57.2	15.2	96.5	ND	ND	ND	ND
2H-3, 45-47	11.95	4.5	0.0	34.3	55.4	10.3	96.5	20.6	56.9	22.5	0.0
2H-3, 123-125	12.73	4.5	0.0	35.8	52.0	12.1	95.6	14.1	65.6	20.3	0.0
2H-4, 45-47	13.45	4.6	0.0	31.5	58.0	10.5	94.2	12.8	62.6	24.6	0.0
2H-4, 123-125	14.23	4.2	0.0	37.2	51.0	11.9	95.7	15.6	63.9	18.6	0.0
2H-5, 45-47	14.95	4.4	0.0	24.4	67.5	8.1	94.4	19.7	59.2	21.1	0.0
2H-5, 123-125	15.73	4.3	0.0	38.0	53.6	8.4	94.0	20.6	59.3	20.1	0.0
2H-6, 45-47	16.45	5.0	0.0	27.1	58.7	14.2	95.6	23.9	60.5	15.0	0.6
2H-7, 45-47	17.45	4.4	5.1	37.4	47.7	9.9	93.9	ND	ND	ND	ND
3H-1, 45-47	18.45	4.5	0.0	33.9	57.7	8.4	94.0	22.7	63.8	13.5	0.0
3H-1, 123-125	19.23	4.6	0.0	28.5	60.9	10.6	92.7	15.3	67.4	17.3	0.0
3H-2, 45-47	19.95	4.7	0.0	26.4	65.4	8.2	93.7	13.9	71.2	14.9	0.0

Notes: ND = no data. HMC = high-Mg calcite, LMC = low-Mg calcite.

Table T5. Grain size, carbonate, and total organic carbon data, Site 1134.

Core, section, interval (cm)	Depth (mbsf)	Mean (ø)	Gravel (wt%)	Sand (wt%)	Silt (wt%)	Clay (wt%)	Carbonate (wt%)	TOC (wt%)
182-1134A-								
1H-1, 45–47	0.45	6.17	1.40	13.43	56.44	28.72	93.22	1.95
1H-2, 45–47	1.95	5.54	0.19	11.85	72.48	15.48	93.24	2.78
1H-3, 45–47	3.45	4.96	1.15	35.55	43.82	19.48	93.16	2.33
2H-1, 45–47	4.95	4.99	0.72	32.47	53.14	13.66	90.70	2.59
2H-2, 45–47	6.45	5.70	6.34	15.66	52.46	25.55	94.47	1.68
2H-3, 45–47	7.95	7.67	1.32	12.56	33.18	52.94	92.74	1.77
2H-4, 45–47	9.45	8.13	0.67	14.81	24.87	59.64	92.21	2.20
2H-5, 45–47	10.95	6.80	4.05	10.11	45.75	40.10	91.97	2.18
2H-6, 45–47	12.45	7.38	0.49	15.24	37.49	46.78	94.52	1.54
2H-7, 45–47	13.95	7.22	0.00	17.52	36.83	45.65	84.21	ND
3H-1, 45–47	14.45	7.11	0.00	11.19	48.42	40.39	83.74	ND

Notes: TOC = total organic carbon. ND = no data.

Table T6. Grain size, carbonate, and total organic carbon, Site 1129.

Core, section, interval (cm)	Depth (mbsf)	Mean (ø)	Gravel (wt%)	Sand (wt%)	Silt (wt%)	Clay (wt%)	Carbonate (wt%)	TOC (wt%)
182-1129C-								
1H-1, 45–49	0.45	3.90	1.51	79.12	13.80	5.57	ND	ND
1H-1, 130–134	1.30	3.73	3.40	61.15	31.72	3.73	94.85	1.31
1H-2, 91–95	2.40	4.61	0.50	47.16	43.24	9.10	92.21	2.50
1H-3, 40–44	3.40	4.84	1.85	44.39	41.90	11.86	83.62	5.15
1H-3, 130–134	4.30	3.35	8.68	57.42	26.15	7.75	94.82	1.35
1H-4, 91–96	5.41	3.74	0.00	69.45	25.63	4.92	95.30	2.09
1H-5, 68–72	6.68	4.36	1.43	62.49	25.98	10.10	ND	ND
2H-1, 45–49	7.75	3.77	4.06	70.70	15.41	9.84	97.45	0.83
2H-1, 122–126	8.52	4.29	4.81	46.60	38.01	10.58	96.62	1.71
2H-2, 72–76	9.52	4.11	2.67	66.09	20.13	11.11	ND	ND
2H-3, 30–34	10.60	4.36	2.11	57.11	30.54	10.23	ND	ND

Notes: ND = no data. TOC = total organic carbon.

Table T7. Grain size, carbonate, and total organic carbon, Site 1131.

Core, section, interval (cm)	Depth (mbsf)	Mean (ø)	Gravel (wt%)	Sand (wt%)	Silt (wt%)	Clay (wt%)	Carbonate (wt%)	TOC (wt%)
182-1131A-								
1H-1, 45–49	0.45	4.50	1.13	59.20	30.16	9.50	76.13	5.34
1H-1, 130–134	1.30	4.51	3.31	45.43	42.72	8.54	76.49	6.93
1H-2, 80–84	2.30	4.77	1.36	44.98	41.82	11.84	75.29	6.00
2H-1, 45–49	3.85	4.70	0.47	36.75	57.13	5.65	92.20	2.19
2H-1, 140–144	4.80	4.83	0.67	45.28	38.34	15.72	ND	ND
2H-2, 45–49	5.35	5.15	1.18	31.24	50.94	16.64	ND	ND
2H-3, 10–14	6.50	6.20	0.78	25.07	45.81	28.34	ND	ND
2H-3, 100–104	7.40	5.99	8.18	47.58	1.97	42.27	96.54	2.04
2H-4, 45–49	8.35	4.63	3.34	38.02	47.21	11.42	98.19	1.12
2H-4, 140–144	9.30	5.65	5.20	26.38	42.74	25.68	ND	ND
2H-5, 96–100	10.36	5.50	1.07	26.88	51.97	20.08	95.67	1.50

Notes: ND = no data. TOC = total organic carbon.

Table T8. Grain size, carbonate, and total organic carbon, Site 1127.

Core, section, interval (cm)	Depth (mbsf)	Mean (ø)	Gravel (wt%)	Sand (wt%)	Silt (wt%)	Clay (wt%)	Carbonate (wt%)	TOC (wt%)
182-1127B-								
1H-1, 45–49	0.45	4.87	4.58	20.59	62.65	12.18	90.99	2.20
1H-1, 140–144	1.40	4.96	4.77	14.67	66.90	13.66	91.43	2.19
1H-2, 100–104	2.50	5.05	3.64	19.24	65.18	11.93	90.26	3.21
1H-3, 41–44	3.41	5.32	1.20	21.87	63.21	13.71	74.91	8.38
1H-3, 130–134	4.30	5.30	0.00	21.48	65.78	12.74	78.95	8.73
1H-4, 90–94	5.40	4.84	0.00	22.52	70.32	7.16	90.11	3.08
2H-1, 47–51	6.45	5.35	0.65	9.68	76.74	12.93	76.56	8.98
2H-2, 20–24	7.60	5.49	0	17.3	68.71	14	86.87	6.14
2H-2, 46–50	7.86	5.44	0.64	24.39	60.31	14.67	91.48	3.48
2H-3, 45–49	9.35	5.58	0.91	20.56	61.76	16.78	91.89	4.44
2H-4, 10–14	10.5	4.91	1.41	37.56	49.54	11.49	ND	ND

Note: ND = no data. TOC = total organic carbon.